Energy-based investigation of multiple liquefaction properties of sand subjected to different strain histories

Enquête sur la base d'énergie de plusieurs propriétés de liquéfaction de sable soumis à différentes histoires de contrainte

Yudai Aoyagi
Department of Civil Engineering, University of Tokyo, Japan, aoyagi@geot.t.u-tokyo.ac.jp

Takeshi Sato
Engineering Department, Integrated Geotechnology Institute, Japan

ABSTRACT: After investigation of liquefaction damage induced by The 2011 of Pacific Coast of Tohoku Earthquake, it was found that liquefaction could occur at multiple times at the same sites. In order to study the multiple-liquefaction properties, in this study, a series of cyclic simple shear tests were conducted on dry Toyoura sand while keeping constant volume of the specimen using of a newly developed stacked-ring shear apparatus. The specimen was subjected to different levels of shear strain during each liquefaction stage. In order to investigate how the occurrence of previous liquefaction may affect the soil behavior during future liquefaction stage, the energy dissipated during the previous liquefaction was separated into positive impact energy and negative impact energy. In addition, different definitions of the threshold condition between the two types of dissipated energy were employed for comparison. The analysis revealed that the two components can be more reasonably evaluated by setting the threshold condition at the state when the effective path passed the phase transformation line for first time.

RÉSUMÉ : Suite à l'enquête effectuée sur le séisme de 2011 de la côte Pacifique du Tohoku, il a été constaté que la liquéfaction pouvait se produire à plusieurs reprises au même endroit. Afin d'étudier les multiples caractéristiques de la liquéfaction, une série d'essais de cisaillement simple cycliques ont été effectués sur du sable de Toyoura. Ces essais ont été effectués à volume constant à l'aide d'un appareil de cisaillement annulaire empilé récemment mis au point. L'échantillon a été soumis à différents niveaux de contrainte de cisaillement au cours de chaque étape de liquéfaction. Afin d'étudier l'impact de précédente(s) liquéfaction(s) sur le comportement du sol lors de nouveaux phénomènes de liquéfaction, l'énergie dissipée précédemment a été séparée en énergie d'impact positive et énergie d'impact négative. De plus, différentes configurations des conditions de seuil entre les deux types d'énergie dissipée ont été utilisées pour la comparaison. L'analyse a révélé que les deux composantes peuvent être évaluées plus raisonnablement en fixant les conditions de seuil à l'état lors duquel le trajet effectif a atteint la ligne de changement de phase pour la première fois.

KEYWORDS: Liquefaction, Re-liquefaction, Cyclic simple shear test, Shear strain history, Dissipated energy

1 INTRODUCTION

According to liquefaction survey after the 2011 Off the Pasific Coast of Tohoku Earthquake (Wakamatsu, 2012), liquefaction damage was found within a 650km long zone that extended in the eastern part of Japan causing extensive damage to residential houses, lifelines and infrastructures. Multiple-liquefaction at the same site was identified where liquefaction had occured at the previous earthquakes. Nevertheless, the mechanisms of multiple liquefaction are not fully understood.

So far, several pioneer works have been conducted to investigate soil behaviors during re-liquefaction using triaxial apparatus (Ishihara and Okada, 1978). However, most of these studies were limited mostly up to 2 stages of liquefaction due to becoming heterogenous specimen after it liquefied.

In this study, investigation of the multiple liquefaction behavior of sand was conducted by using a newly developed apparatus so-called stacked-ring shear apparatus (Wahyudi et al, 2015).

This paper aims to investigate the effects of pre-liquefaction histories with different shear strain amplitudes on the behavior of re-liquagction based on energy dissipated during cyclic loading.

2 STACKED-RING SHEAR APPARATUS

The outline of the stacked-ring shear apparatus is shown in Figure 1a). The axial stress is applied through a pneumatic system using bellofram cylinders, while the torque is controlled by a direct motor system with the maximum and minimum rotation speeds of 64.8deg./min and 0.015deg./min, respectively.

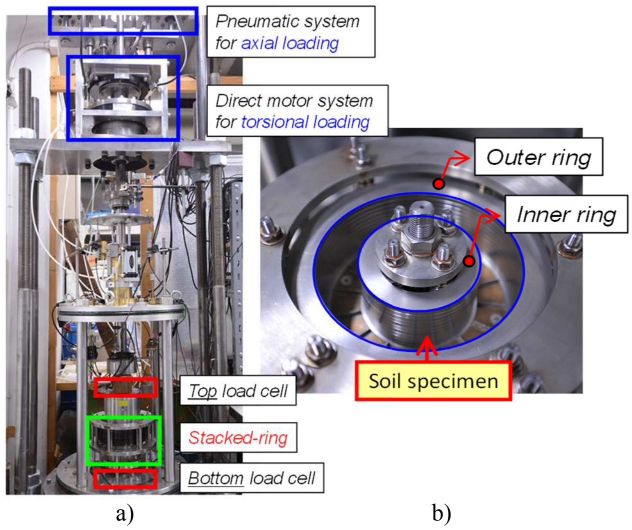

Figure 1. a) Outline of stacked-ring shear apparatus and b) stacked-rings

A hollow cylindrical specimen is placed in between inner and outer parts of the stacked-ring as shown in Figure 1b). The inner and outer diameters of the specimen are 90mm and 150mm, respectively, while the height of the specimen is 55mm.

Both parts of the stacked-ring are composed by 11 pieces of vertically stacked individual rings (thickness is 5mm) with frictionless coating so called Diamond-Like-Coating. Six pieces of metal bearings and four pieces of metal bearings were inserted in between the outer rings and inner rings respectively, so the side wall friction in circumferential direction of rings can be reduced as minimum as possible. A 0.1mm thick annular spacer is inserted on the top of bearings. The 0.1mm thickness of the spacer is large enough to avoid any contact between neighborhood rings, but small enough to prevent the extrusion of the Toyoura sand particles (D_{50}> 0.1mm) during shearing. Each of the rings is free to move individually in the circumferential direction, while top cap was fixed in the vertical direction.

Two bi-component load cells are installed at the top and bottom part of stacked-ring respectively to measure vertical stress and shear stress at the top and bottom of the specimen. The applied stresses in the specimen are solely controlled by the top load cell, while the bottom load cell measures the amounts of transferred stresses.

3 MATERIALS AND EXPERIMENTAL PROCEDURES

Liquefaction tests that use the stacked-ring shear apparatus are conducted on dry specimens under constant-volume conditions. This stems from the assumption that the decrease in applied effective vertical stress (σ'_v) during constant volume shear tests on fully dry specimens has good respondence with the increase pore water pressure (Δu) in undrained shear tests on fully saturated specimens (Finn et al, 1977).

3.1 *Materials*

Dry Toyoura sand was used as the test material. Its physical properties are as follows: specific gravity, G_s= 2.656; mean diameter; D_{50}= 0.210mm; fines content less than 75 µm, F_c= 0.1%; max. void ratio, e_{max}= 0.992; min. void ratio, e_{min}= 0.632. The specimens were prepared by air-pluviation method. The falling height was kept constant throughout the pluviation process to obtain specimens with highly uniform density. All specimens were with initial relative density (Dr_0) around 51%.

3.2 *Experimental procedures*

The procedures to conduct multiple-liquefaction test are as follows:

First, the specimen was consolidated one-dimensionally up to 200kPa of vertical stress ($\sigma_{v.Top}$= 200kPa). Then, each of the specimens was subjected with cyclic shear stress of ±25kPa (τ_{cyc}= 25kPa) with a shear strain rate of 0.7%/min up to pre-fixed maximum shear strain double amplitude (γ_{DAmax}). During the entire shearing process, any vertical movement of the top cap was prevented to simulate simple shear conditions as much as possible.

To investigate the effects of different γ_{DAmax} at each liquefaction stages, the tests were subjected with different maximum shear strain double amplitudes of 2% and 10% on each liquefaction stage. Note that each liquefaction stages were completed by adding another half-cycle of shear loading to bring shear strain back to zero. This was purposely done to prevent any possible additional effects of induced anisotropy while investigating the effects of shear strain amplitude (Ishihara and Okada, 1978).

Next liquefaction stage was started after re-consolidating the liquefied specimen stage into their original $\sigma_{v.Top}$ of 200kPa. The next subsequent liquefaction stages follow the same procedure as the one described in the first liquefaction stage.

In this study, the liquefaction resistance was evaluated by evaluating the number of cycles needed to induce the double amplitude of shear strain 2.0% ($N_{\gamma DA= 2.0\%}$) where shear strain amplitude started to increase rapidly at each liquefaction stage.

4 EXPERIMENTAL RESULTS

A typical liquefaction behavior of Toyoura sand is presented in Figure 2a) and 2b). Figure 2a) shows stress-strain (τ-γ) relationships during liquefaction. The corresponding effective stress path is reported in Figure 2b). It can be seen from Figure 2a) and 2b) that the current test on a dry specimen of Toyoura sand could at least qualitatively reproduce the liquefaction behavior that has been observed in previous studies.

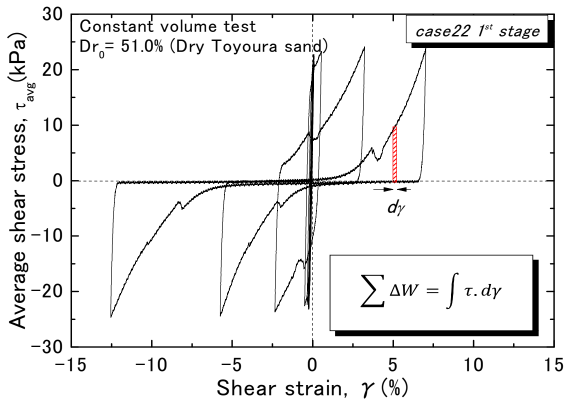

a)

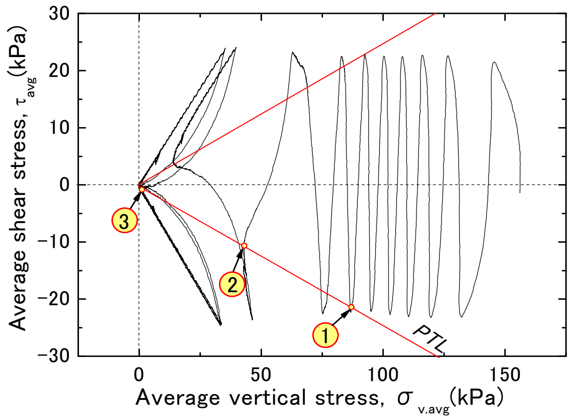

b)

Figure 2. a) Shear stress and shear strain relationship for multiple-liquefaction test and definition of dissipated energy and b) effective stress path and phase transformation line (PTL)

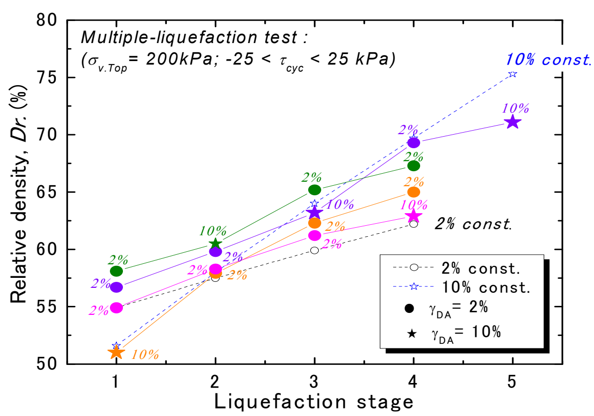

Figure 3. Change in relative density during multiple-liquefaction tests

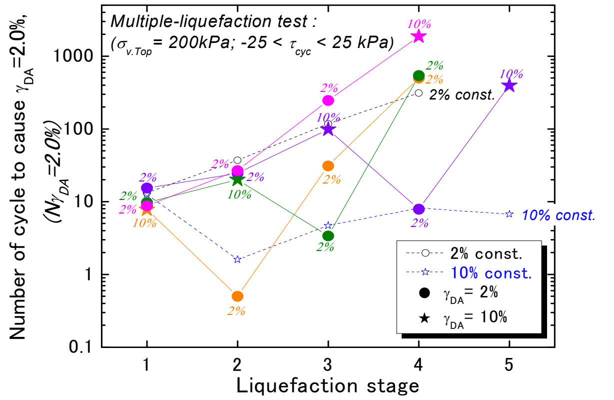

Figure 4. Number of cycles to cause liquefaction during multiple-liquefaction tests

A summary of test results and their comparisons is shown in Figures 3 and 4 for all multiple liquefaction tests. Figure 3 shows the effects of different γ_{DAmax} on the change in relative density (Dr) after reconsolidation for five subsequent multiple liquefaction stages.

The numbers illustrated in the graph are γ_{DAmax} at each liquefaction stages. It can be seen that in all tests, Dr increased gradually, whereas the increment of Dr induced by the liquefaction and reconsolidation stages was larger with higher γ_{DAmax} value. Figure 4 shows the effects of different γ_{DAmax} on $N_{\gamma DA= 2.0\%}$ (the number of cycles needed to induce the double amplitude of shear strain 2.0%) during multiple liquefaction stages. After the specimen was sheared up to γ_{DAmax}= 10%, liquefaction resistance sharply decreased at next liquefaction stage. On the other hand, with the specimen sheared up to γ_{DAmax}= 2%, liquefaction resistance always increased. For comparison, the results of a series of multiple liquefaction subjected with same γ_{DAmax} on each liquefaction stage is also reported as broken lines in Figures 3 and 4. In addition, while the liquefaction resistance decreased only at 2nd liquefaction stage in a series of multiple-liquefaction subjected with same γ_{DAmax} on each liquefaction stage, it decreased even at 4th stage in a series of multiple-liquefaction subjected with different γ_{DAmax} on each stage.

5 METHODOLOGY OF DISSIPATED ENERGY ANALYSIS

Several previous researches have showed that dissipated energy during cyclic loading is related with pore water pressure increment (Kokusho, 2014). There is possibility that the liquefaction potential can be estimated using energy dissipated on each cyclic loading. In this study, in order to investigate how the occurrence of previous liquefaction may affect the soil behavior during future liquefaction stages, detailed analysis of multiple liquefaction tests from viewpoint of dissipated energy during each liquefaction stage was conducted.

The dissipated energy ΔW during each loading cycle was defined as the hysteresis area of the stress-strain (τ-γ) relationship, and its amount $\Sigma\Delta W$ was evaluated as the sum as illustrated Figure 2a). In order to compare the accumulation rate of dissipated energy among different test results, the accumulated shear strain $\Sigma\Delta\gamma$ was evaluated as the sum of the single shear strain amplitude during the cyclic loading stage, as illustrated in Figure 5.

$$\text{Dissipated energy: } \sum \Delta W = \int \tau \ d\gamma \qquad (1)$$

$$\text{Accumulated strain: } \sum \gamma = \int \left|\frac{d\gamma}{dt}\right| \ dt \qquad (2)$$

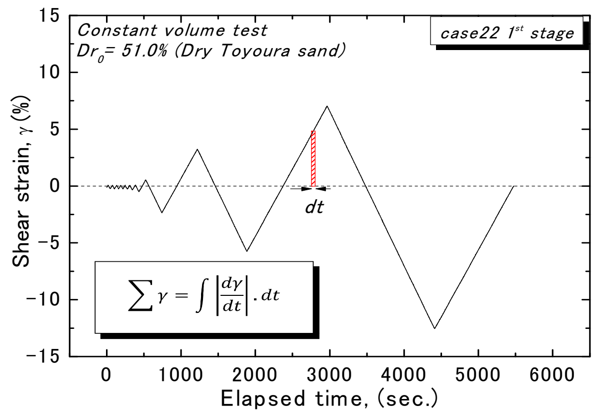

Figure 5. Definition of accumulated shear strain

The shear stress τ is calculated as the average of the stress values at the top load cell and the bottom load cell. As a result, their relationship could be obtained as typically shown in Figure 6. According to previous study (Wahyudi and Koseki, 2015), the stress path during the first liquefaction stage in the test is shown in Figure 2b), on which the following three characteristic states are marked; the stress path first reached the phase transformation line (denoted as PTL hereafter) at state 1; the shear strain amplitude started to increase rapidly after passing state 2; and the vertical stress became zero for the first time at state 3.

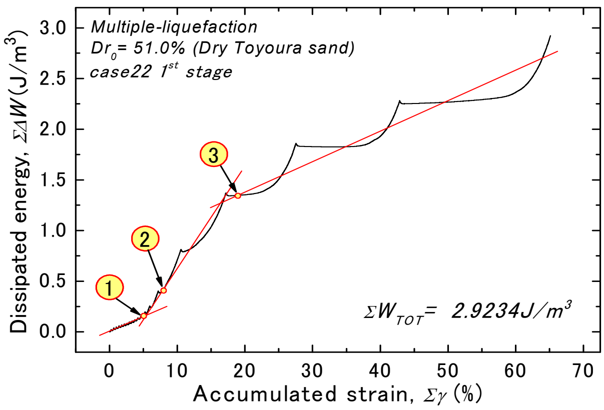

Figure 6. Relationships between dissipated energy and accumulated shear strain

In addition, until reaching state 1, the value of dissipated energy $\Sigma\Delta W$ increased linearly with the accumulated strain $\Sigma\gamma$. After passing state 2, the relationship between $\Sigma\Delta W$ and $\Sigma\gamma$ entered into the second linear region with higher accumulation rate of $\Sigma\Delta W$. After passing state 3, the $\Sigma\Delta W$ and $\Sigma\gamma$ relationship changed again, entering into the third linear region with lower accumulation rate of $\Sigma\Delta W$.

It has been reported by Wahyudi and Koseki (2015) that the energy dissipated during previous liquefaction was separated into two types of components; one with positive impact $\Sigma\Delta W^{(+)}$ and the other with negative impact $\Sigma\Delta W^{(-)}$. A positive impact of dissipated energy causes an increase in the re-liquefaction resistance. On the other hand, a negative impact of dissipated energy resulted in reduction of the re-liquefaction resistance.

In this study, different definitions of the threshold condition between the two types of dissipated energy were employed for comparison. The following two types of analysis were conducted; a positive impact of dissipated energy $\Sigma\Delta W^{(+)}$ was assumed to accumulate only until reaching the state 1 (the stress path first reached PTL) as defined before, while its negative impact $\Sigma\Delta W^{(-)}$ was assumed to accumulate after exceeding this state, in analysis 1; On the other hand, in analysis 2, the $\Sigma\Delta W^{(+)}$ was assumed to until reaching state 2 (γ started to increase rapidly), while its $\Sigma\Delta W^{(-)}$ was assumed to accumulate after exceeding this state.

6 DISSIPATED ENERGY ANALYSIS RESULTS

The value of $\Sigma\Delta W^{(+)}$ and $\Sigma\Delta W^{(-)}$ for analysis 1 and analysis 2 from the multiple liquefaction tests results were evaluated and plotted in Figures 7a) and 7b), together with the $N_{\gamma DA=2.0\%}$ values obtained in the next liquefaction stage.

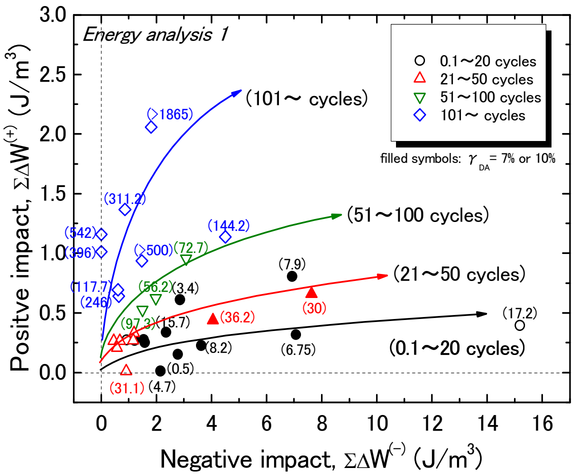

a) Analysis 1

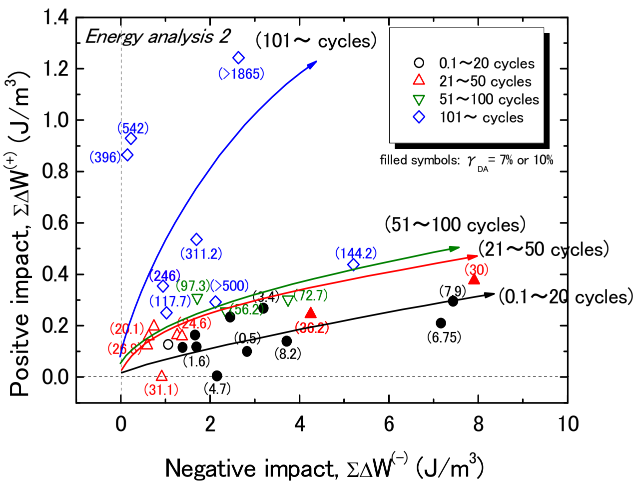

b) Analysis 2

Figure 7. Relationships among positive and negative impacts and the number of cycles in the next liquefaction stage

From these figures, following observations can be made; In both analyses 1 and 2, the $N_{\gamma DA=2.0\%}$ values was decreased with reduction of $\Sigma\Delta W^{(+)}$ and/or increase of $\Sigma\Delta W^{(-)}$. By associating the test data that exhibited similar $N_{\gamma DA=2.0\%}$ values irrespective of the liquefaction stage and different shear strain amplitude, both of the dissipated energy components with positive impacts $\Sigma\Delta W^{(+)}$ and negative impacts $\Sigma\Delta W^{(-)}$ in the previous liquefaction stage affect uniquely the liquefaction resistance ($N_{\gamma DA=2.0\%}$) in the next liquefaction resistance, as typically drawn in Figures 7a) and 7b) for the range of $N_{\gamma DA=2.0\%}$ equal to 0.1~20, 21~50, 51~100 and 101~.

According to the comparison between analyses 1 and 2, the components with positive impacts $\Sigma\Delta W^{(+)}$ and negative impacts $\Sigma\Delta W^{(-)}$ can be more reasonably evaluated by setting the threshold condition at the state when the stress path passed the PTL for the first time (analysis 1). More detailed analysis of the tests results is under way, which will be reported elsewhere in the near future.

However, after applying shear strain histories with its double amplitude exceeding 5% (γ_{DAmax}= 7, 10%; square symbol and star symbol in Figures 7a) and 7b)), the energy-based analysis could not yield a unique relationship between the combination of the dissipated energy components and the liquefaction resistance in the future event. It suggests that proper correction should be applied in evaluating the dissipated energy components.

7 CONCLUSIONS

The following main conclusions can be drawn from the analysis of dissipated energy conducted on results from a series of constant-volume cyclic torsional shear tests subjected to different shear strain amplitudes using stacked-ring shear apparatus:

1) Different definitions of the threshold condition between the two types dissipated energy were employed. In both analyses 1 and 2, the number of cycles needed to induce the double amplitude of shear strain 2.0% ($N_{\gamma DA=2.0\%}$) was decreased with reduction of positive impact $\Sigma\Delta W^{(+)}$ and/or increase of negative impact $\Sigma\Delta W^{(-)}$.

2) Both of the dissipated energy components with positive and negative impacts in the previous liquefaction affect uniquely the liquefaction resistance in the next liquefaction. The components can be more reasonably evaluated by setting the threshold condition at the state when the stress path passed the phase transformation line (PTL) for the first time.

3) After applying shear strain histories with its double amplitude exceeding 5%, the energy-based analysis could not yield a unique relationship between the combination of the dissipated energy components and the liquefaction resistance in the future.

8 ACKNOWLEDGEMENTS

The authors would like to express our gratitude to Professor Junichi Koseki (University of Tokyo) and Dr. Seto Wahyudi for their contributed supports with test data in this paper.
This work was supported by JSPS KAKENHI Grant number 15H04036. The authors acknowledge the supports.

9 REFERENCES

Finn, W. D. L. and Vaid, Y. P. 1977. Liquefaction potential from drained constant volume cyclic simple shear test. *Proc., 6th World Conf. Earthquake Eng.*, Vol.3, 2157-2162.

Ishihara, K. and Okada, S. 1978. Effects of stress history on cyclic behavior sand. *Soils and Foundations* Vol.18, No.4, 69-88.

Kokusho, T., 2014. Liquefaction potential evaluations: energy-based method versus stress-based method, *Canadian Geotechnical Journal*, 50, 1088-1099.

Wahyudi, S., Koseki, J., Sato, T., and Chiaro, G. 2015. Multiple-Liquefaction Behavior of Sand in Cyclic Simple Stacked-Ring Shear Tests, *Int. J. Geomech.*, 10.1061/(ASCE)GM.1943-5622.0000596, C4015001.

Wahyudi, S. and Koseki, J. 2015. Analysis of re-liquefaction prop erties based on energy approach, *Bulletin of ERS*, University of Tokyo, 48, 51-61.

Wakamatsu, K. 2012. Recurrence of liquefaction at the same site induced by 2011Great East Japan Earthquake Compared with Previous Earthquakes. *Proc. of 15th Int'l conf. of Earthquake. Engrg.*